Neuron, Volume *104*

Supplemental Information

Patient-Tailored, Connectivity-Based Forecasts of Spreading Brain Atrophy

Jesse A. Brown, Jersey Deng, John Neuhaus, Isabel J. Sible, Ana C. Sias, Suzee E. Lee, John Kornak, Gabe A. Marx, Anna M. Karydas, Salvatore Spina, Lea T. Grinberg, Giovanni Coppola, Dan H. Geschwind, Joel H. Kramer, Maria Luisa Gorno-Tempini, Bruce L. Miller, Howard J. Rosen, and William W. Seeley

Supplemental Information

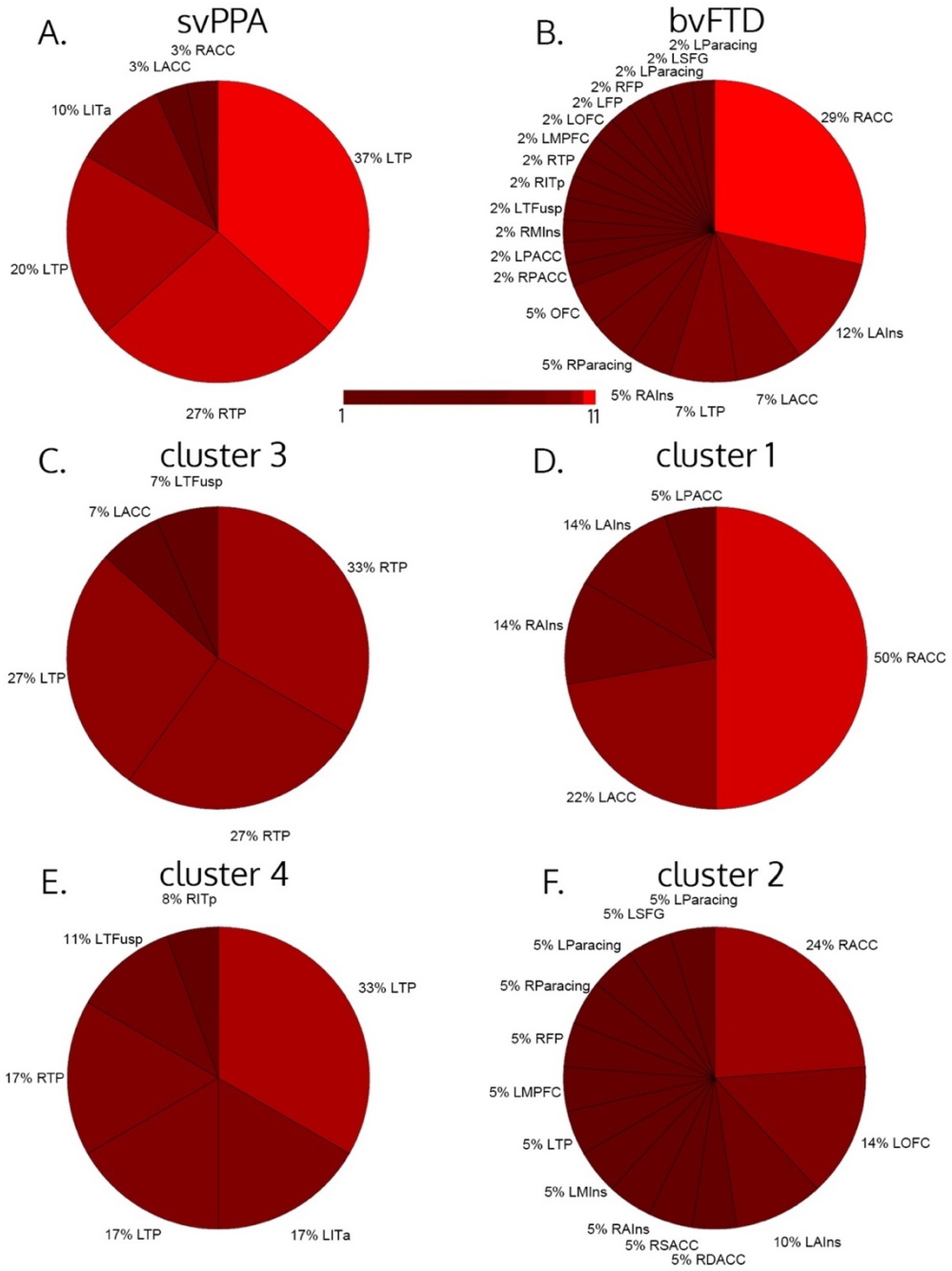

Supplemental Figure 1, Related to Figure 2
Epicenter frequencies by syndrome (A-B) and atrophy cluster (C-F). Counts are only shown for top-ranked epicenter at baseline scan. R: right. L: left. ACC: anterior cingulate cortex. PACC: pregenual anterior cingulate cortex. SACC: subgenual anterior cingulate cortex. DACC: dorsal anterior cingulate cortex.

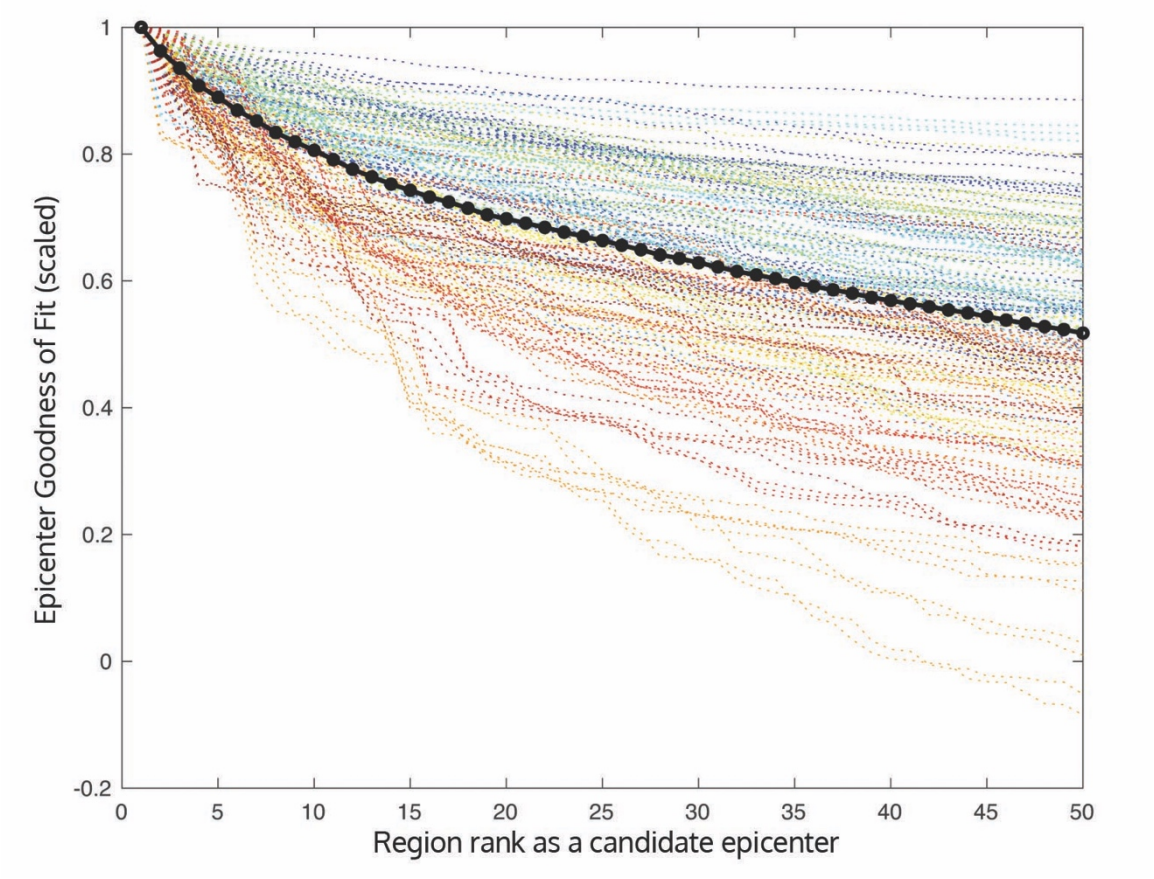

Supplemental Figure 2, Related to Figure 2
Epicenter goodness of fit scores (spatial correlation coefficients) for the top 50 ranked candidate epicenter regions for each of the 235 scans, scaled to the top region's goodness of fit score for that scan. All scans for a given subject are shown in the same color. The black line shows the mean across the 235 scans.

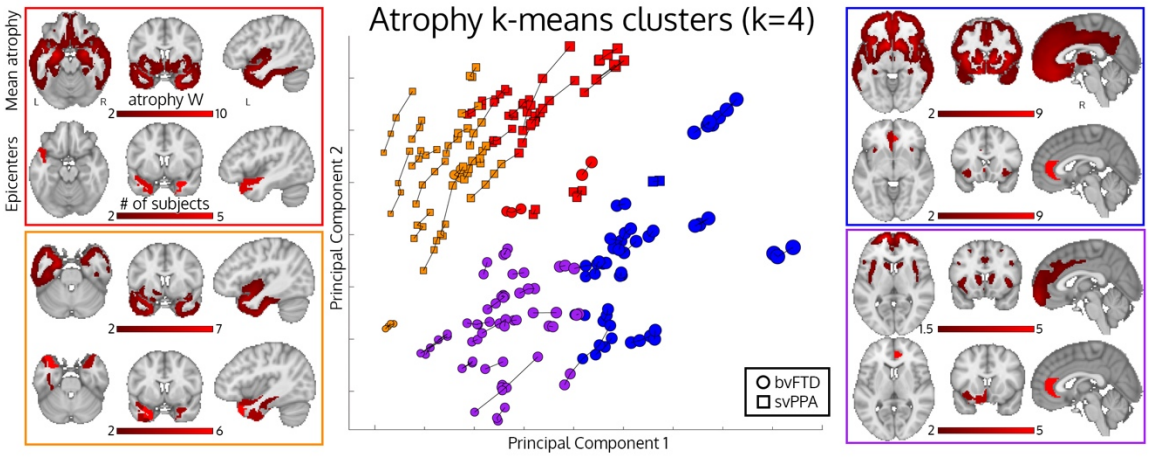

Supplemental Figure 3, Related to Figure 2
Patient baseline atrophy W maps are clustered into 4 groups using PCA and *k*-means clustering (*k*=4). Cluster 1, upper right/blue: y=18, x=2, z=-6; Cluster 2, lower right/purple: y=14, x=2, z=6 (atrophy), y=42, x=2, z=6 (epicenters); Cluster 3, upper left/red: y=6, x=-44, z=-18; Cluster 4, lower left/orange: y=6, x=-40, z=-28. PCA dimensionality reduction yields principal dimensions that primarily map to syndrome localization (x-axis) and atrophy severity (y-axis). Dot radius represents mean level of atrophy across the entire brain. For epicenter locations, see **Supplemental Table 4** and for FTD genetic mutation carriers in each group see **Supplemental Table 5**.

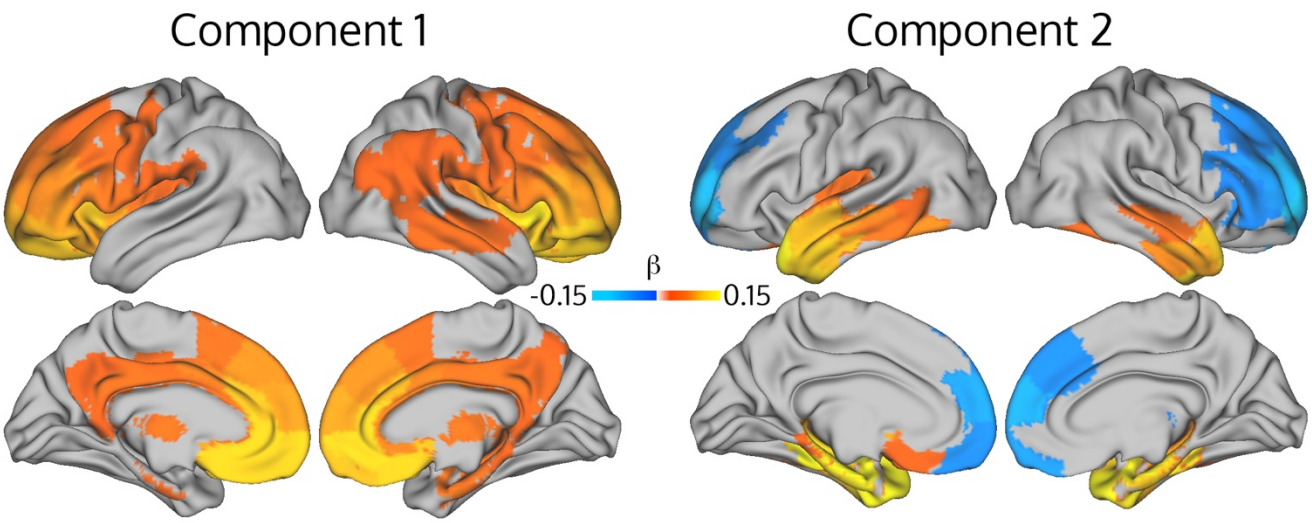

Supplemental Figure 4, Related to Figure 2.
Regional atrophy correlations with component loading scores. For the first two components (see **Figure 2**), a set of regions had significant correlations between region atrophy W score across subjects and component loading score across subjects ($p < 0.0002$, corrected for multiple comparisons, corresponding to $\beta > 0.05$). Component 1 resembles the bvFTD group atrophy pattern, with subjects that are more positive on dimension 1 exhibiting greater atrophy in insular, frontal, cingulate, and subcortical regions. Component 2 resembles the svPPA group atrophy pattern, with subjects that are more positive on dimension 2 showing more atrophy in temporal regions, and elevated gray matter volume in rostral frontal regions.

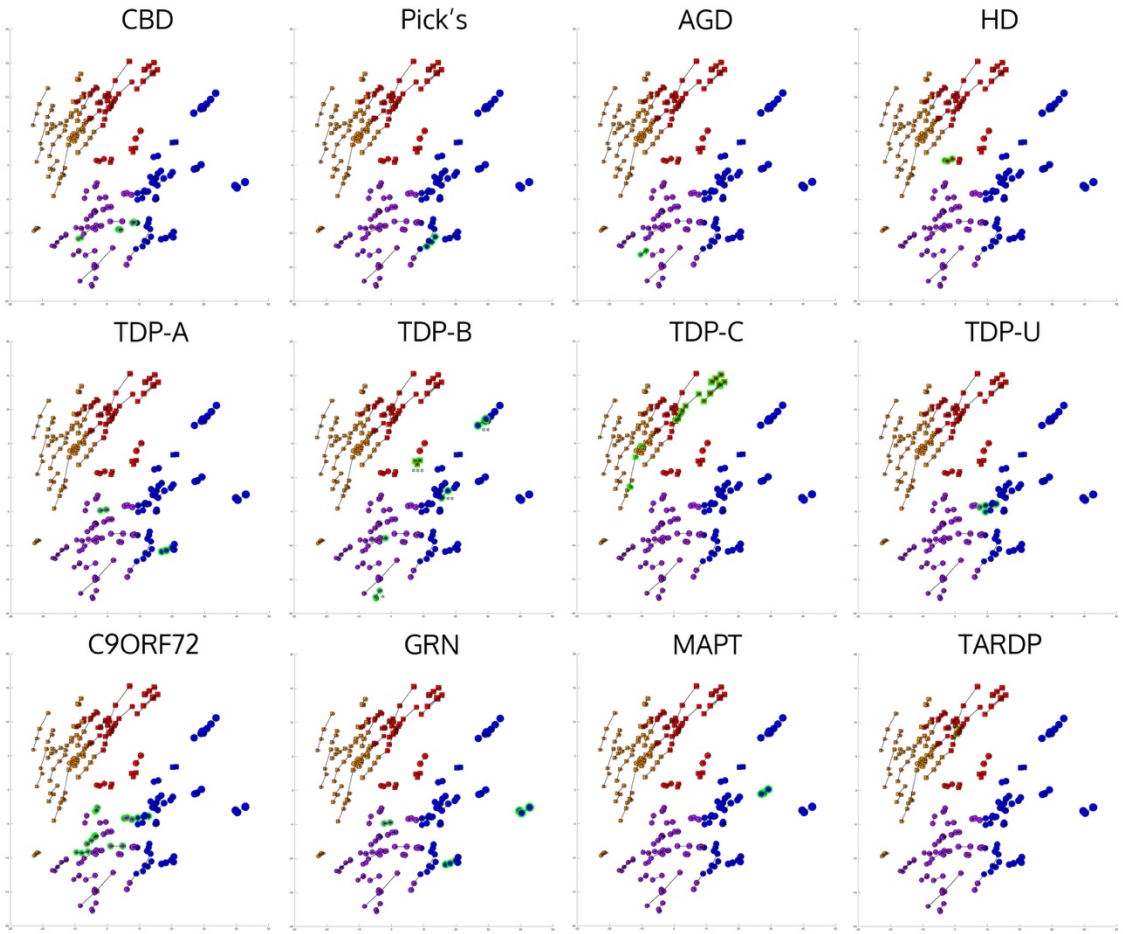

Supplemental Figure 5, Related to Figure 2
Patient baseline atrophy W maps are clustered into 4 groups using PCA and *k*-means clustering (*k*=4). Equivalent to Figure 2, with subjects labeled based on 1) post-mortem pathological diagnosis (rows 1 and 2) or 2) possession of on the major FTLD disease causing mutations. CBD: corticobasal degeneration. Pick's: Pick's Disease. AGD: argyrophilic grain disease. HD: Huntington's Disease. TDP-A: TDP-43 type A. TDP-B: TDP-43 type B. TDP-C: TDP-43 type C. TDP-U: TDP-43 unclassifiable. Among patients with TDP-B, one patient also comorbid amyotrophic lateral sclerosis (*), two patients had comorbid motor neuron disease (**), and one patient had a secondary unclassifiable tauopathy (***).

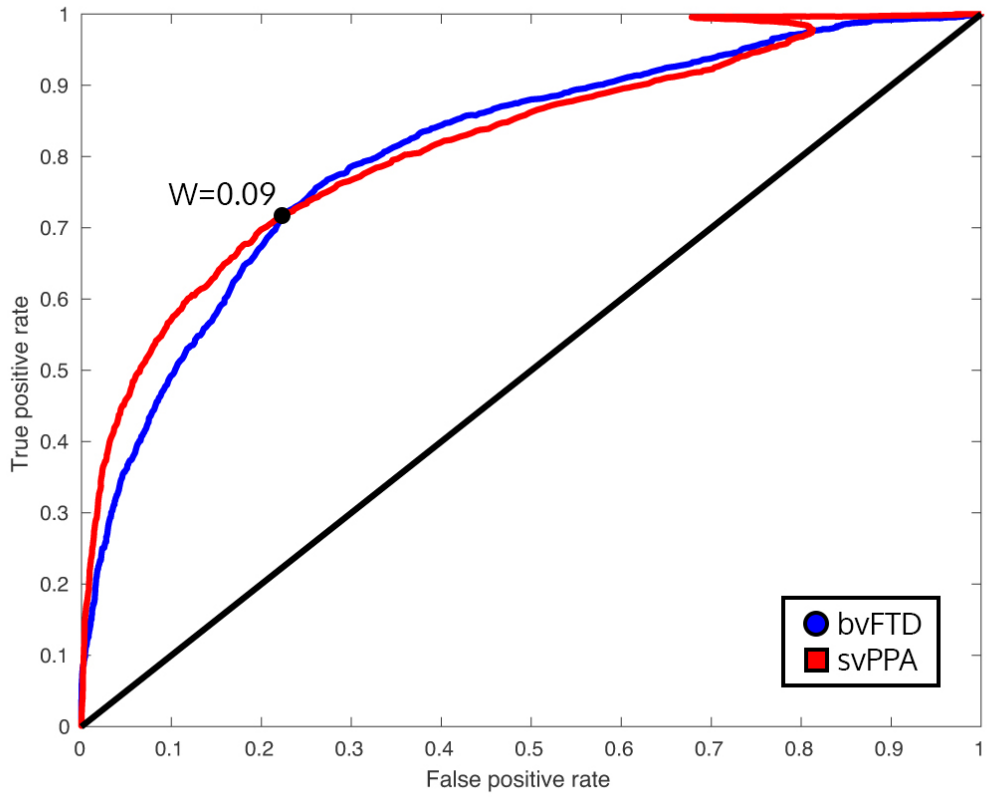

Supplemental Figure 6, Related to Figure 4.
Receiver Operating Characteristic curve of model accuracy in predicting regional longitudinal atrophy. The true positive rate (sensitivity) and false positive rate (1-specificity) were defined by pooling all regions across all subjects within a given syndrome, and assessing the accuracy across the range of longitudinal atrophy values (baseline scan to followup scan W-score change). The area under the curve for patients with bvFTD (AUC=0.81) and svPPA (AUC=0.82) were both substantially greater than chance.

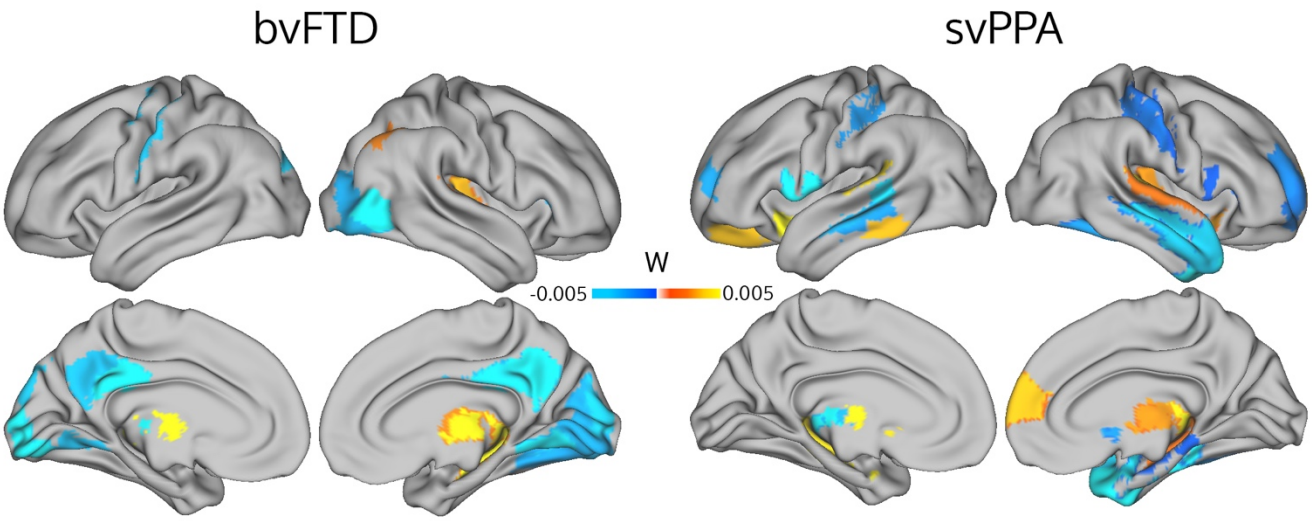

Supplemental Figure 7, Related to Figure 4.
Model prediction errors for network-based and pure spatial spread models. Areas with positive values (red-yellow) are where the spatial model made more accurate predictions (had smaller absolute error) than the network model, while areas with negative values (blue-lightblue) are where the network model made more accurate predictions. The results are shown as group averages across all longitudinal scans from patients with a given a syndrome. In bvFTD (left), the network model made more accurate predictions in areas that were spatially distant from the areas of peak baseline atrophy in the insula (see **Figure 2**), including the posterior cingulate, precuneus, and occipital lobe. The spatial model made more accurate predictions in areas spatially adjacent to the baseline atrophy peak, particularly in the thalamus. In svPPA (right), the network model again made more accurate predictions in areas physically distant from but connectionally adjacent to the baseline atrophy peak in the left anterior temporal lobe (see **Figure 2**), most prominently in the contralateral right anterior temporal lobe along with the somatosensory cortex. The spatial model again made more accurate predictions in subcortical areas such as the striatum and thalamus proximal to the baseline atrophy locations.

Age (years)	66.3 ± 10.8
Sex (F/M)	172/116
Education (years)	17 ± 2
Handedness (R/L/A)	250/35/3
MMSE	29.5 ± 0.7
Field Strength (3T/1.5T)	220/68

Supplemental Table 1, Related to Figure 1
Demographic information for n=288 subjects in structural MRI control set.

Age (years)	65.3 ± 10.0
Sex (F/M)	33/42
Education (years)	17 ± 2
Handedness (R/L)	68/7
MMSE	29.4 ± 0.7
fMRI head max translation, mm	0.62 ± 0.27
fMRI head max rotation, degrees	0.39 ± 0.17
fMRI sum head displacement, mm	42.20 ± 19.82
Number of frames with movement > 1 mm	0.17 ± 0.53

Supplemental Table 2, Related to Figure 1
Demographic information for n=75 subjects in functional MRI control set.

Epicenter region	***n***
bvFTD	
right pregenual anterior cingulate cortex	12
left ventral frontoinsular cortex	5
left pregenual anterior cingulate cortex	3
left dorsal lateral temporal pole	3
right ventral frontoinsular cortex	2
right dorsal medial prefrontal cortex	2
left orbitofrontal cortex	2
svPPA	
left ventral medial temporal pole	11
right ventral medial temporal pole	8
left ventral temporal pole/inferior temporal cortex	6
left ventral temporal pole/fusiform cortex	3

Supplemental Table 3, Related to Figure 2
Epicenter locations and counts for patients with bvFTD and svPPA

Region	MNI coordinate	Peak atrophy W-score
Cluster 1		
Right frontoinsula	36, 16, 0	7.42
Left frontoinsula	-34, 18, -2	6.9
Right caudate	12, 16, -2	8.35
Left caudate	-12, 14, -2	8.65
Left nucleus accumbens	-12, 18, -22	7.89
Left subgenual anterior cingulate	-6, 44, -10	6.35
Cluster 2		
Left frontal pole	-10, 64, -6	4.62
Left frontoinsula	-36, 22, -2	3.19
Right frontoinsula	38, 22, 0	3.08
Left caudate	-12, 14, 6	2.83
Right caudate	12, 16, 4	2.65
Left middle frontal gyrus	-26, 26, 46	2.56
Cluster 3		
Left amygdala	-26, -6, -22	9.82
Right amygdala	26, -4, -22	8.95
Right anterior medial temporal fusiform cortex	26, 0, -42	7.36
Left anterior medial temporal fusiform cortex	-28, -8, -38	7.14
Cluster 4		
Left temporal pole	24, 8, -36	4.42
Right amygdala	-26 -6 -22	7.24

Supplemental Table 4, Related to Figure 2
Epicenter locations for patients with different atrophy subtypes

	GRN	*MAPT*	*C9orf72*	*TARDP*
Cluster 1	2	1	0	0
Cluster 2	1	0	6	0
Cluster 3	0	0	0	1
Cluster 4	0	0	0	0

Supplemental Table 5, Related to Figure 2
Number of patients with FTD-causing genetic mutations for different atrophy subtypes

Cluster ID/descriptor	n	Mean CDR-SB	Regions	Epicenters
1/bvFTD severe	18	6.7	Anterior cingulate, insula, frontal, and temporal lobes	Anterior cingulate and insula
2/bvFTD moderate	21	6.3	Insula, rostral/orbital frontal lobe, and caudate	Anterior cingulate, insula, and frontal lobe
3/svPPA severe	15	4.0	Bilateral temporal	Left/right anterior temporal
4/svPPA moderate	18	3.3	Left temporal	Left anterior temporal

Supplemental Table 6, Related to Figure 2
Description of different atrophy subtypes based on k-means clustering (k=4).

	Mode	Median	Mean	Range
Subsequent rank of the original baseline epicenter out of 194	2	2	2.9	2-21
Baseline rank of regions that were subsequently "promoted" to epicenter	2	2	2.6	2-6

Supplemental Table 7, Related to Figure 2
Epicenter location stability within subjects longitudinally
For subjects where different epicenter locations were identified at different timepoints, the subsequent ranks of original epicenter and baseline ranks of regions that become epicenter. 52 subjects had identical epicenters detected at each of their longitudinal time points (31/42 bvFTD, 21/30 svPPA), while 20 subjects had non-identical epicenters at two or more time points. In the majority of cases the epicenter identification differences at different timepoints were extremely minor.

	Original model F-statistic	Alternative model F-statistic
Baseline atrophy	F=118.62	F=82.99
Nodal hazard	F=73.53	F=30.04
Euclidean distance to epicenter	F=73.84	F=86.36
Shortest path to epicenter	F=80.87	F=72.32
Spatial hazard	F=N/A	F=92.21

Supplemental Table 8, Related to Figure 4
Model comparison for models with or without spatial hazard
Individual term F-statistics for the single-epicenter network-based model and an alternative model that includes an individual term for spatial hazard.